THE ASTROPHYSICAL JOURNAL, 338:1094–1105, 1989 March 15

RADAR OBSERVATIONS OF COMET HALLEY

D. B. CAMPBELL AND J. K. HARMON
National Astronomy and Ionosphere Center
AND
I. I. SHAPIRO
Harvard-Smithsonian Center for Astrophysics
Received 1987 December 21; accepted 1988 August 18

ABSTRACT

Radar observations of comet Halley were made with the 12.6 cm radar at the Arecibo Observatory during the comet's 1985 inbound Earth approach. A weak (9 σ) echo was detected, making Halley (at a geocentric distance of 0.63 AU) the most distant comet yet detected with radar. The echo spectrum was dominated by a broad-band feature whose high radar cross section (32 ± 10 km^2) and large Doppler bandwidth (approximately 100 Hz) are inconsistent with an echo from the nucleus. An inferred upper limit of 0.045 for the radar albedo of the nucleus implies a surface of relatively high porosity. A plausible source of the observed echo is backscatter from large (>2 cm radius) grains ejected from the comet's surface. This would make Halley the second comet (after IRAS-Araki-Alcock) to yield a radar detection from large grains. The required number density of large grains in the Halley coma is reasonable in light of the results for IRAS-Araki-Alcock and given the fact that, of the two, Halley was much the more active comet. The inferred grain population is also consistent with particle detector measurements made during the Halley spacecraft encounters.

Subject headings: comets — radar astronomy

I. INTRODUCTION

Comets, being small objects, are difficult to detect with Earth-based radar. The first radar detection of a comet (Encke) was not made until 1980 (Kamoun *et al.* 1982), and only three other comets had been detected as of 1985 (Ostro 1985). All four of these comets yielded a narrow-band Doppler spectrum attributable to backscatter from a single, small (kilometer-size) nucleus. One of them (comet IRAS-Araki-Alcock [IAA]) exhibited an echo with an additional broad-band component which was subsequently identified with scattering from large (centimeter-size) grains ejected from the nucleus (Campbell *et al.*, 1983; Shapiro *et al.* 1983; Goldstein, Jurgens, and Sekanina 1984; Harmon *et al.* 1989).

The two most distant comets to be detected were Encke and Grigg-Skjellerup. Both objects were observed at a geocentric distance of 0.33 AU and yielded weak detections (less than 10 σ) after several hours of integration distributed over a number of days (Kamoun *et al.* 1982; Kamoun 1983). Observations of several other comets at comparable distances failed to yield detections. Given this experience, and the fact that the radar echo strength varies as the inverse fourth power of the distance, the chances for a radar detection of comet Halley during its recent apparition were considered to be marginal. The best opportunity for observing Halley from Arecibo was during its close approach to Earth on the inbound portion of its passage around the Sun late in 1985 November, when the geocentric distance was 0.62 AU. Unfortunately, Halley was not within the Arecibo telescope's limited declination coverage during its closer (0.42 AU) approach to Earth during its outbound passage in 1986 April.

Despite the poor observing opportunity, a series of S-band (2380 MHz, $\lambda = 12.6$ cm) radar observations was conducted at Arecibo during Halley's inbound pass, and a weak echo was detected. The Halley echo was unusual for its high radar cross section and large bandwidth. The weakness of the detection precludes a detailed analysis and conclusive interpretation of the results. It is possible, however, to place some constraints and to draw some preliminary conclusions from a comparison of the Arecibo results with other Earth-based Halley observations, the Halley spacecraft encounters, and the radar results for comet IAA.

II. OBSERVATIONS

The radar observations were made during the hours 0000–0400 UT on five dates in 1985: November 24, 28, and 29 and December 1 and 2. During this period the geocentric distance of Halley varied between 0.62 and 0.64 AU, and the heliocentric distance decreased from 1.59 to 1.47 AU. The relevant radar system parameters were 465 kW, 71 dB, and 35 K for the transmitter power, antenna gain, and system temperature, respectively. From four to six transmit/receive cycles were made on each of the five dates. Each cycle contained a transmit and a receive period, each of 10 minute duration, the round-trip light-travel time. The total on-source receive integration time for the five days was 4.1 hr. In addition, off-source test observations of half-hour durations were made on three of the five days to monitor the spectral characteristics of the receiver noise.

A right-circular polarized (monochromatic) continous wave (CW) was transmitted, and both right- and left-circular polarizations were received. The abbreviations OC (opposite circular) and SC (same circular) will be used to denote, respectively, the received polarization senses which are the opposite of, and the same as, the transmitted sense. The OC ("polarized") echo has the same sense as that for specular reflection by smooth surface undulations, whereas the SC ("depolarized") echo is generally associated with multiple scattering or with single scattering by wavelength-scale structure. Most planetary radar targets, including asteroids, return much more OC than SC power. This characteristic was also found in

the echoes from each of the three other comets (IAA, Grigg-Skjellerup, Sugano-Saigusa-Fujikawa) detected with dual-polarization radar systems (Kamoun 1983; Campbell *et al.* 1983; Goldstein, Jurgens, and Sekanina 1984; Harmon *et al.* 1989). A highly polarized echo is also expected for single scattering from particles or grains which are small with respect to the wavelength of the radar. Scattering from such particles ejected from the surface of the comet's nucleus by outgassing is thought to be responsible for the broad-band component in the echo spectrum for comet IAA (Campbell *et al.* 1983; Shapiro *et al.* 1983; Goldstein, Jurgens, and Sekanina 1984; Harmon *et al.* 1989).

The signal for each polarization channel was coherently converted to base band (0 Hz), low-pass filtered, and quadrature sampled at a 2 kHz continuous rate. The (complex) samples were recorded on magnetic tape for later analysis. Compensation for frequency offsets and drifts, caused by the changing relative velocities of the nucleus and the radar, was performed in real time by means of a computer-controlled local oscillator using frequencies derived from an ephemeris of the comet's motion. This scheme is nominally intended to mix the echo down to base band; however, to avoid any possible confusion between true echo power and spurious direct current or low-frequency power introduced in the postdetection stages, we offset the transmitter frequency by either +400 Hz (November 24) or +212 Hz (all other days). These offsets were later removed in generating the final echo spectra.

III. DATA ANALYSIS AND RESULTS

The data were Fourier-analyzed to yield power spectra with a full bandwidth of 2 kHz and a resolution of 1.95 Hz. By making the appropriate weighted summations of the spectra corresponding to each 10 minute receive period, average spectra (in each sense of received circular polarization) were produced for each of the five days on which observations were made. A spectrum (in each polarization) was also produced corresponding to the average of all data acquired over the five days. The accuracy of the ephemeris of the comet's motion was adequate to allow such averaging without appreciable smearing of the spectra. Since both the size and the spin vector of the nucleus of Halley were unknown at the time of the observations, the bandwidth of any echo could not be predicted. Optimum detection requires smoothing of the spectra with a function having the same spectral shape as that of the expected echo. As an approximation to this, the 1.95 Hz resolution average spectra were smoothed (i.e., convolved) with a $[\sin(\pi f/f_w)/f]^2$ function for a variety of values of the effective bandwidth (or equivalent resolution) f_w. We smoothed by factors of 2^n, where $n = 1, 2, 3, 4, 5, 6$ (corresponding to equivalent resolutions f_w of 3.9, 7.8, 15.6, 31, 62, and 125 Hz). As f_w was varied, the resulting smoothed spectra were inspected for spikes or "bumps" which may have indicated the presence of an echo. The narrowest possibly significant feature found in the Halley spectra was a 15 Hz wide bump seen on December 1. However, the echoes for most of the days also showed a hint of a very broad (a few tens of Hz) bump at the frequency predicted by the ephemeris for an echo from the comet. Subsequent analysis suggested that this broad feature indeed represented an echo from the comet.

Figure 1 shows the five-day-average OC spectrum for various smoothings. Prior to summing, the spectrum from November 24 was shifted by 212–400 = −188 Hz to make it

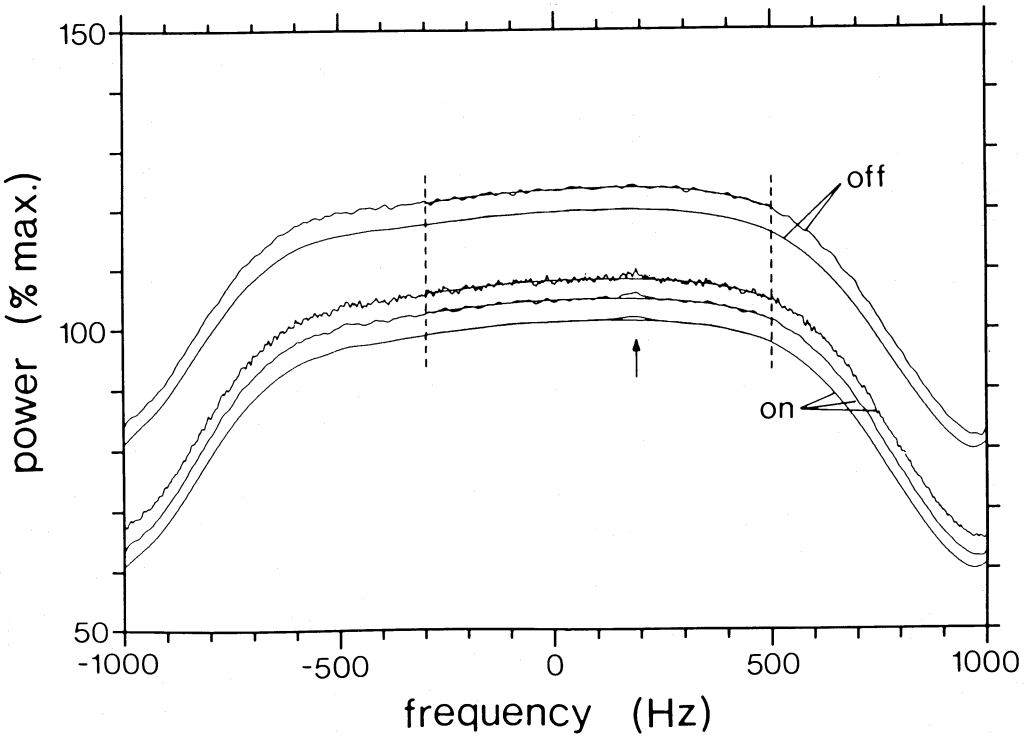

FIG. 1.—Five-day-average power spectra for the Halley observations in the OC sense of polarization and the average OC spectra for all the "off-source" data showing the full 2 kHz passband and the low-pass filter rolloff. The spectra are smoothed to equivalent resolutions of 3.9, 15.6, and 62 Hz (on-source) and 15.6 and 62 Hz (off-source). A polynomial has been fitted to the band between the dashed lines. The arrow indicates the expected frequency (+191 Hz) of the echo from the nucleus. Because arbitrary vertical shifts have been made to separate the spectra for clarity, the absolute vertical scale is only approximately correct for each individual spectrum.

consistent with the transmitter frequency offset of 212 Hz used on the other four days (see § II). In Figure 1 we denote the expected echo frequency as +191 Hz rather than +212 Hz. The 21 Hz difference represents the average discrepancy between the Doppler shifts for the nucleus predicted by the ephemeris used for the observations and the more accurate values from an ephemeris developed in mid-December of 1985. Since the ephemeris discrepancy varied from day to day, small shifts were made to the average spectrum for each day to make the predicted echo center frequency consistent with the nominal +191 Hz offset. The Doppler predictions based on the second ephemeris were estimated to be accurate to within several Hz.

Also shown in Figure 1, for comparison, is the OC off-source spectrum. Because the off-source observations were not simultaneous with the on-source observations and were made on only three of the five observing days, the mean off-source spectrum cannot provide a precise replica of the background noise passband. It can, however, be used to check for the presence of spurious, stable bumps in the receiver passband introduced in the intermediate-frequency (IF) and base-band sections of the receiver system (e.g., in the IF amplifiers and low-pass filters); the introduction of narrow spectral features in the receiver front end would appear to be very unlikely given the large instantaneous bandwidth of the receiver and the smearing effect of the programmed local oscillator drift. The mean off-source spectrum shown in Figure 1 was formed by summing the three OC noise test spectra (from November 28 and December 1 and 2) along with the November 28 OC noise test spectrum shifted by −188 Hz and the SC noise test spectrum from December 2. The shifted November 28 spectrum was included to provide an estimate of the shifted background noise component for November 24, whereas the SC spectrum from December 2 was included as an additional independent estimate of the OC noise bandpass for the previous days (since the IF and base-band electronics for the two polarization channels were purposely interchanged for the final day's observations). This scheme for summing the off-source spectra gave a much more faithful reproduction of the five-day-average on-source noise passband than did a simple summation of the three off-source spectra, because this sum took account of, and attempted to give proper weight to, the frequency shift on November 24 and the anomalous shape of the bandpass on December 1 (when the shape of the low-pass anti-aliasing filter was set incorrectly).

Because the off-source spectrum did not provide a precise replica of the on-source background noise passband (see above), direct subtraction of the off-source from the on-source spectrum was not feasible. Instead, we elected to fit low-order polynomials to the on-source and off-source spectra separately and compare the results. The spectra in Figure 1 were least-squares fitted with a fifth-order polynomial over the 800 Hz span between −300 and +500 Hz. Tests showed that a fifth-order polynomial was the lowest order one capable of following the long-wavelength shape undulations. Since the polynomial was intended to describe the system-noise background only, the 110 Hz section of the on-source spectrum centered on the expected echo frequency of +191 Hz was excluded from the fit; this section was also excluded for the fit to the off-source spectrum to test for possible fit-induced oscillations over the blanked-out section. The fits are very good, with a reduced chi-square of 1.02 and no evidence for fit-induced artifacts. We therefore adopted this fitting scheme to remove the background-noise baselines from all the daily-average and five-day-average spectra.

The on-source spectrum in Figure 1 shows a broad, weak bump at the expected echo frequency. No such feature can be discerned in the off-source spectrum. In Figures 2*a* and 2*b* are shown, respectively, the unsmoothed (1.95 Hz resolution) OC and SC spectra with the background noise baseline removed. Here the +191 Hz offset has been removed so that the expected central frequency of the echo is at 0 Hz. In Figure 2*a* one can discern a small but obvious bump centered approximately on this frequency. The radar cross section computed by integrating over this OC spectral feature is 32 km^2, with an estimated standard error of 6 km^2. Figure 2*c* shows the result of an alternative method of estimating the noise baseline. Here a nonlinear least-squares fit was made to 300 Hz of the unsmoothed OC spectrum using a model of a Gaussian signal plus a quadratic noise baseline. The radar cross section found from the integral over the fitted Gaussian was 32 ± 9 km^2, in agreement with the cross section obtained from the other algorithm; the higher statistical standard error probably resulted from the additional degree of freedom introduced by simultaneous estimation of the signal feature and the noise baseline. The errors quoted above for the cross section do not include errors in calibration of the radar. These are usually estimated to total approximately 25% of the measured cross-section value and, when combined in a root-sum-square sense with the statistical standard errors from the fitting procedures, result in standard errors in the cross section of 10 and 12 km^2, respectively, for the two techniques. Figure 2*d* shows the unsmoothed OC off-source spectrum from Figure 1 with the fitted baseline subtracted in an identical manner to that for Figure 2*a*. Note that this spectrum shows no sign of the feature seen in the on-source spectrum of Figure 2*a*. We subjected the off-source spectrum in Figure 2*d* to a chi-square test for a normal, zero-mean probability density (the distribution expected from the central limit theorem if the polynomial baseline fit is good). This test showed that there was a probability of 59% that the variance would be at least as large as that measured. A similar test of the OC on-source spectrum in Figure 2*a* (with no blanking out of the presumed echo feature) gave a corresponding probability of only 9%, a result which we attribute to "contamination" of the noise spectrum by a real (echo) signal.

The statistical significance of the putative echo feature is best seen from the smoothed spectrum in Figure 3*a*. It was found that the statistical significance of the five-day-average OC echo was maximized when the spectrum was smoothed by a factor of 32 (for an equivalent resolution of 62 Hz). The peak of the smoothed OC spectrum is 8.8 noise standard deviations. An SC feature with about half this strength can also be seen. Because of the discreteness of the trial smoothing factors (see above), the quoted 8.8 standard deviations for the OC detection is probably a slight underestimate. The Gaussian fit in Figure 2*c* gives a full width at half-power of 42 Hz, whereas the smoothing function $[\sin(\pi f/f_w)/f]^2$ has a full half-power width of 52 Hz. From this we conclude that our quoted detection value probably underestimates an optimal (matched-filter) detection by about 10%. Figure 3*b* shows the off-source spectra smoothed in the same way as the spectra in Figure 3*a*; note that these spectra are featureless at the 2.5 σ level and do not exhibit any bumps at the frequency of the putative on-source echo feature.

In Figure 4 we show the average spectra for each of the five days after smoothing at the same equivalent resolution which

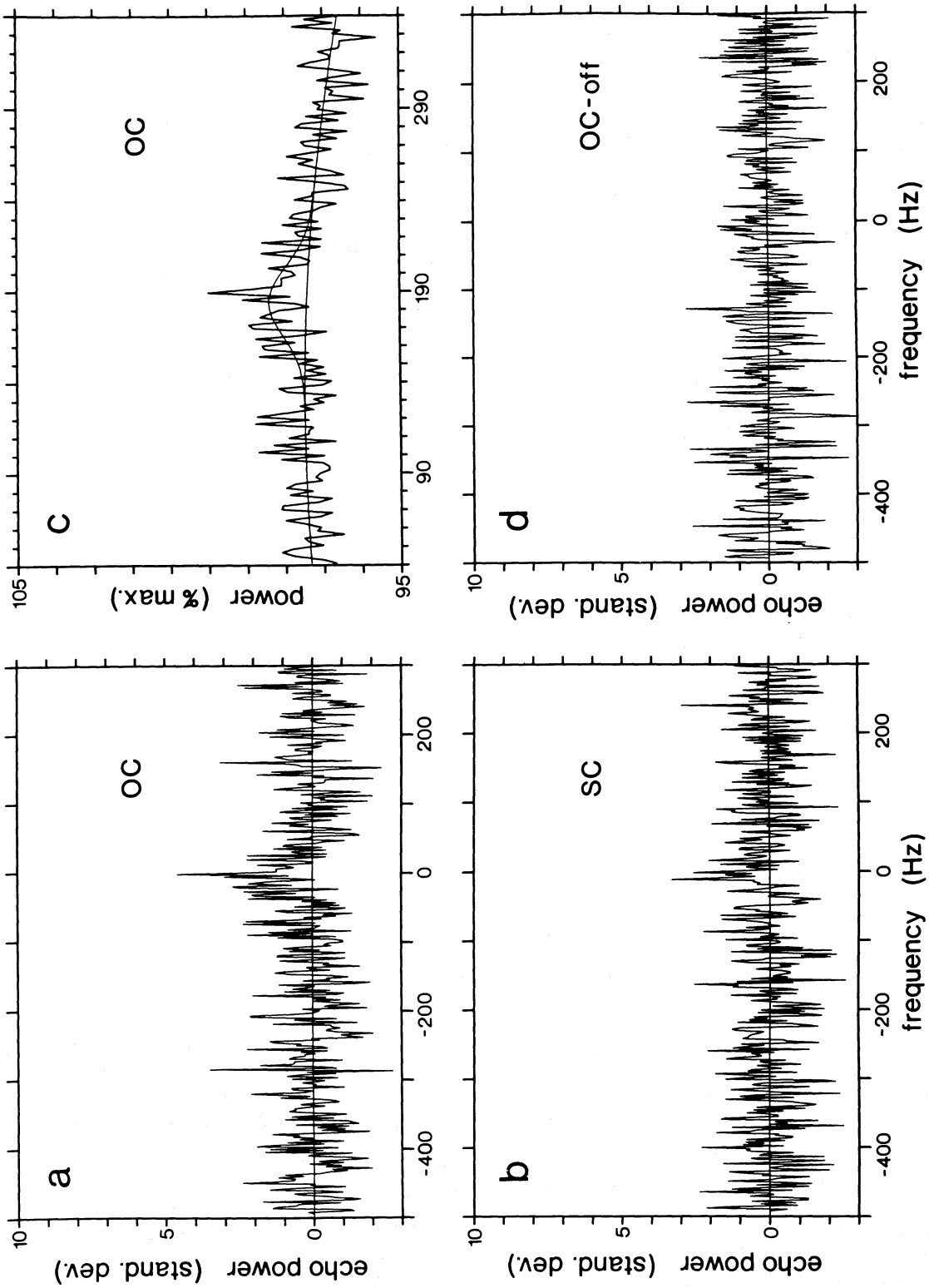

FIG. 2.—Unsmoothed (1.95 Hz resolution) five-day-average spectra with the polynomial fit to the baseline removed: (*a*) OC on-source; (*b*) SC on-source; (*d*) OC off-source. Also shown is (*c*) the five-day-average OC spectrum showing the least-squares fit of a Gaussian echo signal plus quadratic noise baseline. All of the plots except (*c*) have had the +191 Hz offset removed so that 0 Hz represents the expected echo frequency.

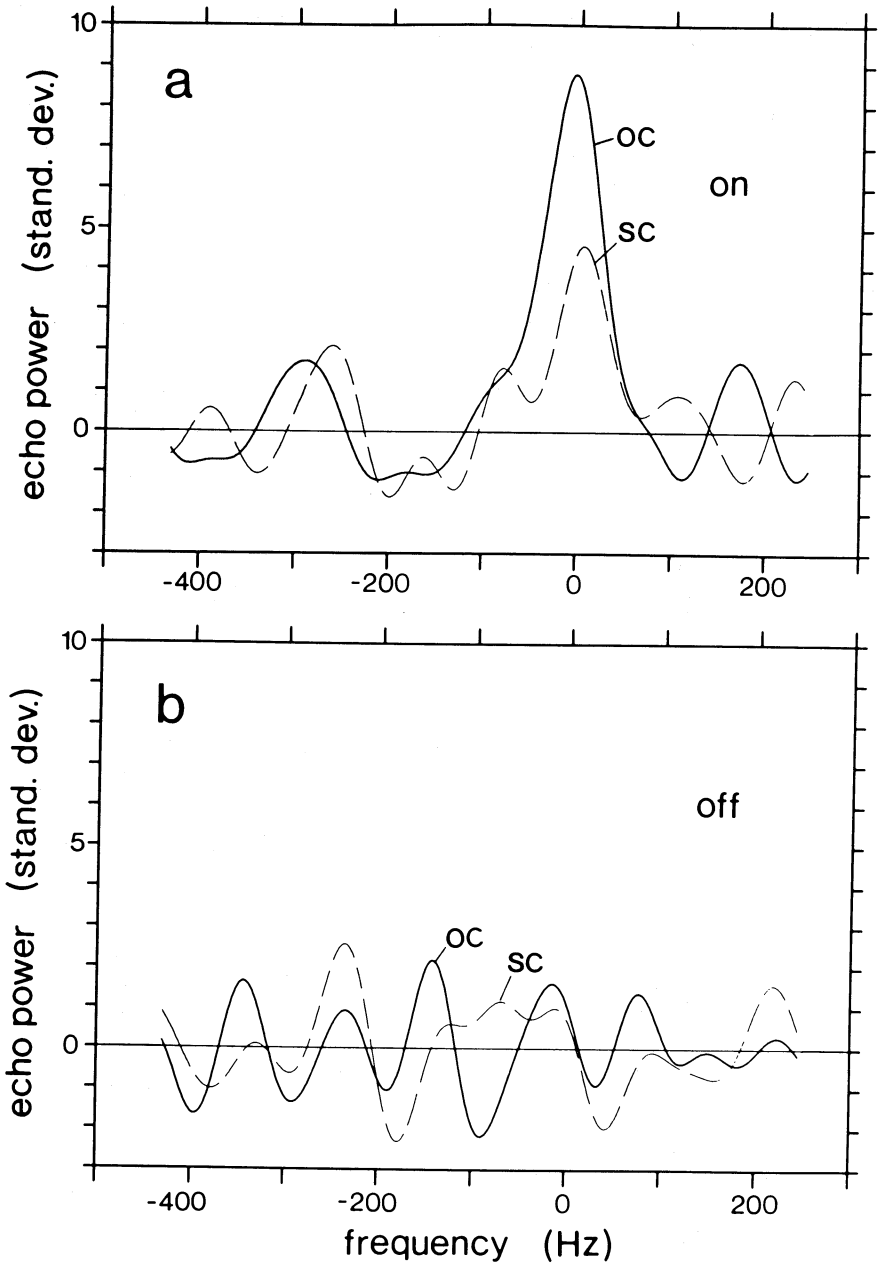

FIG. 3.—Five-day-average OC and SC spectra smoothed to an equivalent resolution of 62 Hz: (*a*) on-source; (*b*) off-source. The +191 Hz offset has been removed so that 0 Hz represents the expected echo frequency.

optimized the detectability of the echo in the five-day-average spectrum. There is evidence for an OC feature near 0 Hz on every day except November 28. The lack of a detection on this day may not be significant in light of the fact that, of the four transmit/receive cycles made on that date, one was made at a zenith angle where the overall system sensitivity is relatively low and another was made at a time when there was suspected to have been an error in telescope pointing. It is somewhat more difficult to explain the echo feature of December 1 being significantly narrower than that seen on the other days. For this day the smoothing which maximized the significance of the echo peak corresponded to a value of f_w of 15.6 Hz. The spectrum resulting from this smoothing can be seen in Figure 4*e*.

On the basis of the foregoing results, we believe it very likely that we have detected radar echoes from comet Halley in the OC polarization. We summarize the supporting evidence for this admittedly weak detection as follows:

1. There is a statistically significant (8.8 σ) bump in the spectrum which is centered within a few hertz of the expected echo frequency.
2. The off-source spectrum does not show this feature, which suggests that the feature which we identify as an echo is very unlikely to be a bump in the background noise spectrum or an artifact introduced in the baseline fitting.
3. The echo feature was evident in the average spectrum on four out of five observing days.
4. The echo power is predominantly in the OC ("expected") polarization.

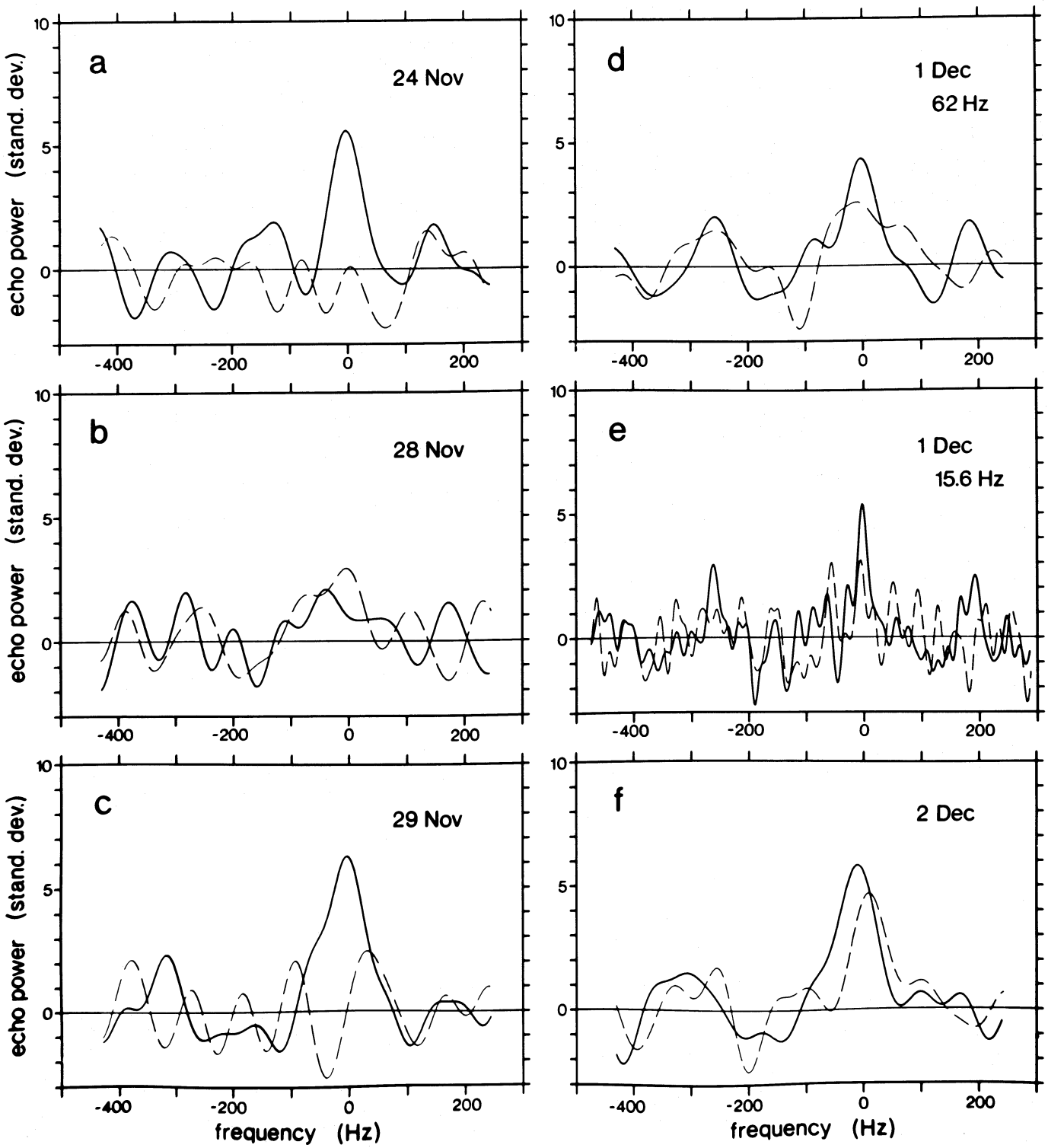

FIG. 4.—Daily-average OC (*solid lines*) and SC (*dashed lines*) spectra smoothed to 62 Hz equivalent resolution: (*a*) November 24; (*b*) November 28; (*c*) November 29; (*d*) December 1; (*f*) December 2. Also shown is (*e*) the December 1 spectra smoothed to 15.6 Hz equivalent resolution.

IV. INTERPRETATION

In evaluating the Halley radar results, the first possibility to be considered is that the echo was returned from a single rotating nucleus. The limb-to-limb bandwidth f_0 of a rotating spherical nucleus is given by

$$f_0 = \frac{8\pi R v \sin i}{c\tau} = \frac{2.3R(\text{km}) \sin i}{\tau(\text{days})}, \quad (1)$$

where R is the nucleus radius, v is the transmitted radio frequency (2380 MHz for the Arecibo radar system), τ is the rotation period, and i is the inclination angle of the rotation axis to the line of sight. Results from the spacecraft encounters indicate that the nucleus is an oblong object with dimensions of approximately 15 × 8 km (Keller *et al.* 1986; Sagdeev *et al.* 1986). The best current estimate of the rotation period is 2.2 days, a figure which was arrived at independently from *Suisei* spacecraft observations of Lyα brightness variations (Kaneda *et al.* 1986*a*, *b*), analysis of dust features in photographs of the 1910 apparition (Sekanina and Larson 1984), and *Vega* spacecraft images (Sagdeev *et al.* 1986). Although more recent papers have debated the possibility of an additional longer period (7.4 day) component to the rotation (Smith *et al.* 1987; Sekanina 1987; Wilhelm 1987), there is general agreement that the dominant contributor to the spin vector is a 2.2 day rotation (or nutation) about the short axis. Values of 50° and 45° for the right ascension and declination of the pole direction, respectively, obtained by Wilhelm (1987), imply a near-constant inclination angle i of 66° during the period of the Arecibo observations. Insertion of these values for the rotation period and inclination angle into equation (1) results in an aspect-dependent bandwidth f_0 of 4–7 Hz, which is much narrower than the bandwidth of the observed echo feature. The high radar cross section also poses problems for the nucleus-echo hypothesis. The measured radar cross section σ of 32 km^2 and an estimated mean projected area A of 80 km^2 gives a radar albedo σ/A of 0.4, a value which seems unreasonably high. This albedo would be much higher than the radar albedo of 0.03 estimated for the nucleus of comet IAA on the assumption (supported by thermal emission data) that IAA had a mean radius of about 5 km (Harmon *et al.* 1988). If the radar backscatter from the Halley nucleus were dominated by specular reflection (which seems to have been the case for IAA), then we can estimate the Fresnel reflection coefficient ρ_0 using $\rho_0 \cong \sigma/gA$, where g is the backscatter gain. Adopting as a reasonable guess $g = 1.5$ (see Harmon *et al.* 1989), we have $\rho_0 = 0.27$ or a dielectric constant of about 10. Thus, the Halley nucleus would have to have a radar reflectivity greater than that of most solid rocks in order to give the measured radar cross section. We conclude that, unless the size and period estimates are grossly in error, the broad-band feature dominating the Halley echo could not have come from the nucleus. We cannot, however, readily dismiss the possibility that the relatively narrow feature seen on December 1 is a nucleus echo observed when the oblong Halley nucleus was at some favorable observing aspect.

The lack of a clear detection of the nucleus allows us to place some bounds on its radar reflectivity. We have found that a broad-band echo with a full bandwidth of approximately 100 Hz and a radar cross section of 32 km^2 gives an 8.8 σ detection. Since the optimum detectability of an echo for a given cross section is inversely proportional to the square root of its bandwidth, then the radar cross section for a 4 σ detection is about $1.5f_0^{1/2}$ (km^2), where f_0 is the echo bandwidth. Using a mean f_0 of 5.5 Hz, we conclude that the radar cross section of the nucleus must have been less than 3.5 km^2. Then, using $A = 80$ km^2 and $g = 1.5$, one can place approximate upper limits of 0.045, 0.03, and 2 for the radar albedo, reflectivity, and dielectric constant, respectively. These limits imply that the Halley nucleus has a high-porosity surface such as a deep snow layer. A similar conclusion was reached for comet IAA based on a comparison of radar results with the best estimates of the nucleus size for that comet (Harmon *et al.* 1989).

The relatively large bandwidth and radar cross section of the Halley echo, features which are difficult to explain on the basis of a nucleus echo, are both easily understood if the echo is predominantly from large grains surrounding the nucleus. The frequency offset Δf from a radial velocity difference ΔV between, say, a grain and the nucleus is given by $\Delta f = (2v/c)\Delta V$, so that at our observing frequency of 2380 MHz one has a frequency dispersion of 16 Hz for each meter per second of velocity dispersion. Thus, relative velocities of only a few meters per second are required to explain the observed bandwidth. Terminal ejection velocities of this magnitude would be expected for centimeter-size grains ejected from the nucleus surface by gas mass fluxes $>10^{-5}$ g cm^{-2} s^{-1} (Goldstein, Jurgens, and Sekanina 1984; Harmon *et al.* 1989). Gas fluxes of this magnitude have in fact been estimated for active regions of the Halley nucleus from analyses of photographs from the 1910 apparition (Sekanina and Larson 1984). There will also be an additional component to the Doppler broadening of the echo spectrum due to variations in the line-of-sight radial velocity across the finite angular extent of the echo-producing region. This "geometric" component (see Harmon *et al.* 1989) can be appreciable if the reflecting grains extend over a significant portion of the radar beam. Given the geocentric orbital velocity of about 30 km s^{-1} for Halley at the time of the radar observations, any grains at the edge of the 2′ (half-power width) Arecibo beam would have had frequency offsets of 100 Hz from this effect alone. Because of the high cross-sectional area-to-volume ratio of grains relative to that of the nucleus, large radar cross sections can be achieved without invoking an unreasonably high total mass in particles. However, this is true only if the largest particles are not significantly smaller than a wavelength, since the backscatter efficiency Q_b of a particle of radius a falls steeply according to the Rayleigh law $Q_b \propto a^4$ for $a < \lambda/2\pi$. If all particles are in the Rayleigh size regime, then a power-law distribution of particle sizes with a total radar cross section of σ would have a total mass given by (see the Appendix for the derivation and assumptions)

$$M \cong \frac{1}{3}\sigma\rho\left(\frac{\lambda}{2\pi}\right)^4 \left|\frac{\epsilon+2}{\epsilon-1}\right|^2 \left(\frac{7-\alpha}{4-\alpha}\right)\left[1-\left(\frac{a_0}{a_m}\right)^{4-\alpha}\right] a_m^{-3}, \quad (2)$$

where ρ and ϵ are the particle density and dielectric constant, respectively; α is the power-law exponent for the particle size distribution ($n \propto a^{-\alpha}$), and a_0 and a_m are the minimum and maximum particle radii, respectively. Taking $\alpha = 3.0$ (see discussion of *Giotto* spacecraft results below) and assuming the particles are solid ice ($\rho = 0.9$ g cm^{-3}, $\epsilon = 3.3$), we find that $M \cong 3 \times 10^{13} a_m^{-3}$ g, where a_m is in centimeters. For $a_m = \lambda/2\pi = 2$ cm, one has $M = 4 \times 10^{12}$ g, which is significantly less than the approximate 5×10^{17} g mass of the nucleus for a mean density of 1 g cm^{-3}. Making $a_m > 2$ cm has little effect because of the turnover in Q_b in the Mie regime. On the other hand, making $a_m < 0.5$ mm gives a total mass in particles greater than the mass of the nucleus itself, a clearly unacceptable result.

The suggestion that most of the Halley echo arises from large grains is motivated by, and invites comparison with, the radar results for comet IAA. The broad-band "skirt" echo from IAA has been identified with backscatter from centimeter-size grains (Shapiro *et al.* 1983; Goldstein, Jurgens, and Sekanina 1984; Harmon *et al.* 1989). The various features of the IAA skirt spectrum were found to be consistent with a model in which large grains are ejected from the nucleus by the same gas-drag mechanism used to explain the ejection of the smaller particles making up the dust coma and tail (Shapiro *et al.* 1983; Harmon *et al.* 1989). The IAA skirt echo had a radar cross section of approximately 0.8 km^2, which is significantly less than the Halley cross section. If Halley were ejecting large grains in a manner similar to that of IAA, then, since Halley was a much more active comet than IAA in terms of gas and dust production, we infer that Halley was also the more active comet in terms of large-grain production. IAA was found to be a dust-poor comet from infrared observations of the dust coma; a total particle production rate of $(1–2) \times 10^5$ g s^{-1} was estimated from an extrapolation of the infrared-derived micron-scale particle population to centimeter scales (Hanner *et al.* 1985). IAA was also a relatively gas-poor comet, with an estimated mass-loss rate in gas of 6×10^5 g s^{-1} at the time of the close Earth passage (Feldman, A'Hearn, and Millis 1984; Hanner *et al.* 1985). Halley was known to be the brightest of the short to medium-period comets and was, therefore, predicted to show relatively high gas and dust production rates during its recent apparition (Divine *et al.* 1986; Weissman and Kieffer 1981; Meier and Keller 1985). This prediction was borne out by reports of Earth-based observations made during Halley's 1985 inbound passage. Infrared observations of the dust coma gave an estimated 2×10^6 g s^{-1} for the mass-loss rate in dust at the time of the Arecibo observations, increasing to 6×10^6 g s^{-1} at a heliocentric distance of 1.0 AU (Hanner 1986; Tokunaga *et al.* 1986). Halley's estimated inbound gas production rate was also high, increasing from 1.2×10^6 g s^{-1} at 2.5 AU (Feldman and Festou 1985) to 1.5×10^7 g s^{-1} at 1.0 AU (Feldman 1986; Wycoff 1986). Similar results were obtained for the outbound passage, when a gas production rate of 1.7×10^7 g s^{-1} was inferred for a heliocentric distance of 0.85 AU (Festou *et al.* 1986). Thus, Halley was roughly 30 times more "active" than IAA for a given heliocentric distance and about 10 times more active than IAA at the respective times of the Arecibo observations. Another factor that may have contributed to the large radar cross section of Halley relative to that of IAA is the 20 times larger diameter subtended by the Arecibo telescope beam at the distance of Halley over that for IAA. Since the transit time for a centimeter-size grain across this beam at the distance of Halley would have been long ($\sim$100 days), possible grain evaporation and the dependence of comet activity on heliocentric distance would tend to reduce the effect of the different beam sizes to a factor well below 20. On the other hand, there would not appear to be any problem in explaining the relative radar cross sections of the Halley and IAA broad-band echoes by invoking a combination of higher grain production rate, larger beam size at the comet, and (given that Halley was observed 0.5 AU farther from the Sun than IAA) lower grain evaporation rate.

The results of the spacecraft encounters offer support for the notion that there were large grains in sufficient quantities to give a detectable radar echo. The *Giotto* images showed that the gas and dust emission was concentrated in several highly collimated jets emanating from a few discrete sources on the nucleus (Keller *et al.* 1986). This collimation implies that the mass fluxes of gas must have been in excess of the 10^{-5} g cm^{-2} s^{-1} required to strip centimeter-size grains from the nucleus. Further, both the *Suisei* and *Giotto* spacecraft suffered impacts with large particles. *Suisei* was hit during its close approach to the comet by two particles of several milligrams mass (presumably millimeter-sized), a surprising result given the large (1.5×10^5 km) cometocentric distance of the spacecraft (Hirao and Itoh 1986). *Giotto* was struck by one relatively large (40 mg) particle which must have measured several millimeters in size (Reinhard 1986; McDonnell *et al.* 1986), whereas an earlier prediction had estimated the probability of an impact with a particle with mass greater than 10 mg as only 13% (Divine *et al.* 1986). Thus, the presence of relatively large particles in the coma of Halley is confirmed, and in numbers which were possibly higher than expected. This is also consistent with the submillimeter particle size distribution function inferred from the *Giotto* and *Vega* measurements (Reinhard 1986; McDonnell *et al.* 1986; Vaisberg *et al.* 1986; Mazets *et al.* 1986), which was found to be flatter than that assumed in making the dust-hazard predictions (Divine *et al.* 1986). The *Giotto* dust detectors gave a spectral index of $\alpha = 3.0$ for the particle size distribution in the vicinity of the spacecraft for mass $m < 10^{-5}$ g, which (because of the $a^{-1/2}$ size dependence of grain velocity) corresponds to a spectral index for the size distribution of the particles at ejection of 3.5 (McDonnell *et al.* 1986). A mass ejection rate of 3×10^6 g s^{-1} was estimated for particles with mass $m \leq 3 \times 10^{-3}$ g by extrapolating from 10^{-5} g using the measured power-law index (McDonnell *et al.* 1986). Extrapolating even further to the centimeter-size ($a_m = 2$ cm) particles that would yield the observed radar echo gives a mass ejection rate of 1.4×10^7 g s^{-1}. If we assume an inverse-square heliocentric distance dependence for the ejection rate, then we can deduce a mass-loss rate in particles from the nucleus of 5×10^6 g s^{-1} at the time of the Arecibo observations. Above, we gave $M = 4 \times 10^{12}$ g as the estimate of the mass in particles required by the measured total radar cross section for $a_m = 2$ cm. These two numbers combined correspond to a mass ejection rate in particles of $\dot{M} = 4 \times 10^7 \tau^{-1}$ (g s^{-1}), where τ is the mean particle lifetime or residence time (in days) in the region about the comet of a size corresponding to that encompassed by the angular extent of the Arecibo beam at the epoch of the radar observations. If $\tau = 100$ days, the expected transit time for a centimeter-size grain across this region, then a mass-loss rate of 4×10^5 g s^{-1} would suffice to give the measured radar cross section. This rate is well below the 5×10^6 g s^{-1} rate found from the power-law extrapolation of the *Giotto* dust measurements, and leaves some margin for a reduced particle lifetime resulting from possible grain evaporation. This argument is presented somewhat more completely in Figure 5. Here we show curves of $\dot{M}(a_m)$ calculated for several particle compositions using the expression given in the Appendix. Also shown is the $\dot{M} \propto a_m^{1/2}$ line giving the mass-loss rate inferred from an extrapolation of the *Giotto* dust-detector data using $\alpha = 3.5$. Note that for $a_m > 2$ cm the *Giotto*-inferred grain ejection rate is well in excess of that required to give the measured radar cross section. Since the $\dot{M}(a_m)$ curves assume a filled beam, the effective diameter of the grain cloud could have been a factor of 4–30 times smaller (depending on composition) than the width of the Arecibo beam and still have yielded the measured radar cross section. This reduced cloud size corresponds to a radius in the range 700–5000 km. Again, we point out that one might expect an unfilled beam because of the

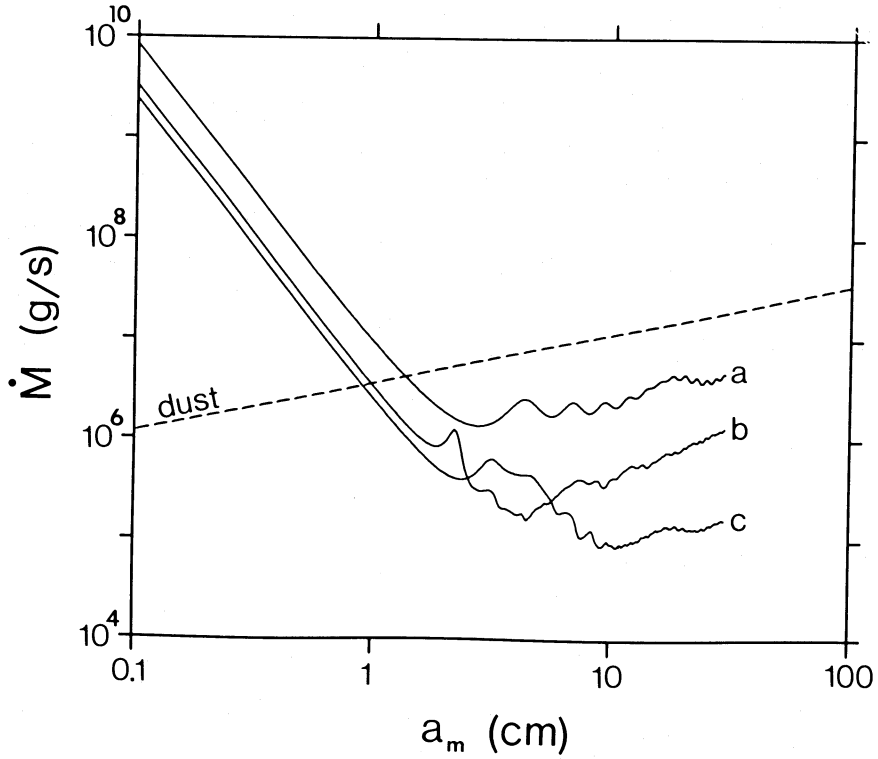

FIG. 5.—Nucleus mass-loss rate (*solid lines*) in particles for an $\alpha = 3.5$ power-law size distribution with a cutoff radius of a_m. The curves were calculated using Mie theory and eq. (A9) assuming $\rho_n = 1.0$ g cm^{-3}, $R = 5$ km, $b = 2 \times 10^4$ km, and $\sigma = 32$ km^2. The curves represent different particle compositions: (*a*) snow, $\epsilon = 1.44$, $\rho = 0.3$ g cm^{-3}; (*b*) rock, $\epsilon = 6.5$, $\rho = 3.0$ g cm^{-3}; (*c*) ice, $\epsilon = 3.3$, $\rho = 1.0$ g cm^{-3}. The values for the imaginary part of the refractive index (m_i) used in the calculations were 0.01 for snow and ice and 0.03 for rock. Shown for comparison is a line $\dot{M} \propto a_m^{1/2}$ (*dashed line*) giving the estimated mass-loss rate from an extrapolation of the *Giotto* dust distribution function.

effects of grain evaporation and of a decrease in cometary activity with increasing heliocentric distance. However, if the grains are made up of a nonvolatile material, then Figure 5 suggests that they must have been rather less dense (and, hence, less reflective per unit mass) than solid rock (see Harmon *et al.* 1989). This is plausible in light of some current theories which claim that cometary grains are fluffy structures with densities of about 0.2 g cm^{-3}.

Passive radio observations are also relevant to this discussion of particle size distributions. Altenhoff *et al.* (1986) have reported detections of radio continuum emission from Halley; they measured flux densities of 5.9 and 52 mJy at $\lambda = 3.5$ and 1.3 mm, respectively. They argued that nucleus thermal emission cannot account for these flux densities, and hence, that the continuum emission must have been dominated by thermal radiation from large grains. Using an expression given in the Appendix, we calculated the 3.5 mm radio continuum flux density (Fig. 6) that one would have expected to measure given the measured radar cross section. The curves in Figure 6 were computed under the assumption that the radar and radio continuum observations were measuring the same population of particles. Thus, since the Arecibo beam was 3 times wider than the beam for the radio continuum observations, the curves in Figure 6 actually represent upper limits. However, the foregoing results suggest that the large-grain cloud probably did not fill the Arecibo beam, so it is likely that the curves in Figure 6 overestimate the predicted continuum flux by a factor which is somewhat less than the ratio of the beam sizes. Although the predicted continuum flux density is very sensitive to the assumed particle conductivity, Figure 6 shows that the radio and radar detections are at least consistent with each other for plausible assumptions about the conductivity. We can also conclude from this figure that one must have $a_m > 1$ cm in order for the predicted radio continuum flux density not to exceed the measured value.

Finally, we discuss two features of the Halley echo which might pose problems for the particle-echo hypothesis or at least stretch the analogy with the IAA skirt echo. The first is the possibility, hinted at by the SC feature in the spectrum, that the Halley echo was much more strongly depolarized than was the IAA skirt echo. The Halley SC feature (Fig. 3*a*) is too weak to claim as a detection but too strong to dismiss outright. The IAA skirt echo showed unusually weak ($\sim 1\%$) depolarization, a result which we used to set an upper limit of several centimeters for the particle cutoff size a_m (Harmon *et al.* 1989). In that paper it was also shown that the depolarization tends to rise dramatically from the Rayleigh value of $<2\%$ to 10% or more as one increases a_m beyond some value (depending on composition) of the order of, or larger than, $\lambda/2\pi$. Hence, if the Halley SC detection were real, then the particle-echo hypothesis would require that the limiting grain size be somewhat larger for Halley than for IAA. A larger limiting size is certainly plausible given the simple gas-drag theory of grain ejection, which has $a_m \propto \dot{\mu}/R$, where $\dot{\mu}$ is the gas flux and R is the mean nucleus radius (Harmon *et al.* 1989). Halley and IAA are believed to be about the same size and, given the likelihood that Halley (being much the more active comet) had a significantly higher $\dot{\mu}$ than IAA, it is probable that Halley was emit-

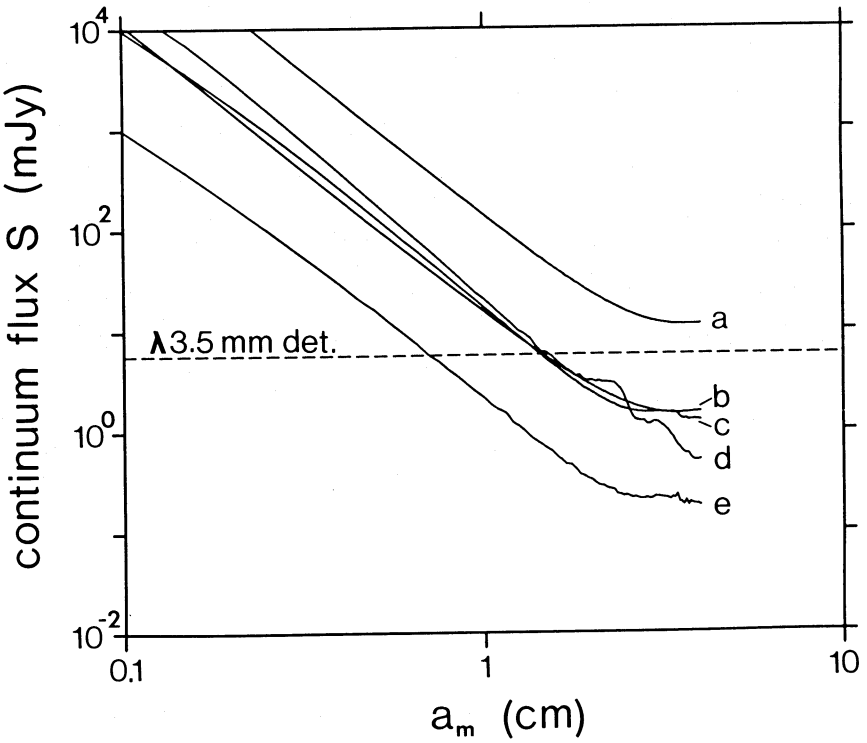

FIG. 6.—Predicted 3.5 mm radio continuum flux (*solid lines*) from thermal emission by particles. The curves were computed from Mie theory and eq. (A11) assuming $\alpha = 3.5$, $T = 200$ K, and $\sigma = 32$ km^2. The particle compositions are as in Fig. 5, but with different values of the imaginary part (m_i) of the refractive index: (*a*) snow, $m_i = 0.01$; (*b*) snow, $m_i = 0.001$; (*c*) ice, $m_i = 0.01$; (*d*) rock, $m_i = 0.03$; and (*e*) ice, $m_i = 0.001$. Shown for comparison (*dashed line*) is the measured flux of the 3.5 mm radio continuum detection by Altenhoff *et al.* (1986).

ting larger grains. The second possible problem arises from the fact that the broad feature in the Halley echo spectrum is centered at approximately −4 Hz, i.e., it is slightly redshifted relative to the expected echo frequency for the nucleus. Calculations along the lines of those described in Harmon *et al.* (1989) show that, given the orbital geometry at the time of the Arecibo observations, the echo from grains ejected preferentially in the sunward direction would have been blueshifted by several hertz relative to the nucleus. A comparison of these results suggests either that large grains from Halley were not concentrated precisely in the sunward direction or that the Doppler ephemeris for the nucleus has an error of the order of 10–20 Hz.

V. CONCLUDING REMARKS

Five nights of Arecibo radar observations of comet Halley revealed a feature in the overall average spectrum which, though weak, seems consistent with being an echo from the comet. The large radar cross section and large bandwidth of this feature suggest that the echo is predominantly from large (>2 cm radius) grains which have been ejected from the nucleus. Extrapolation of the dust particle size distribution to large grain sizes gives a sufficient number of grains to account for the Arecibo echo, although the radar data obviously do not contain enough information to support any model with certainty. The lack of a detectable echo from the nucleus, combined with estimates of its size and rotation rate from the spacecraft encounters and other data, indicate that the nucleus has a surface of relatively high porosity.

The Arecibo detection of a radar echo from Halley is an important result, since it is the first for a "bright' comet and corresponds to by far the largest radar cross section measured to date for a comet. If our interpretation of the echoes is correct, Halley is the first comet to give a stronger echo from particles than from the nucleus itself. These considerations should enhance the prospects, and alter the observing strategies, for future radar observations of bright comets. Halley is not unusually active as bright comets go, so it should be possible to detect grain-cloud echoes from other bright comets at geocentric distances in excess of 0.5 AU. It would be particularly interesting to observe a bright comet at heliocentric distances well under 1 AU, where increased cometary activity might compensate for large geocentric distances. However, opportunities for observing particle echoes from bright and/or close-approaching comets within the next few years will necessarily depend on the chance appearance of objects in the "new" or long-period classes.

We would like to thank the staff of the Arecibo Observatory (NAIC) for their support of these observations. We would also like to thank D. Yeomans for providing the initial conditions on which both sets of ephemerides were based, J. Chandler for computing the ephemerides, and T. Hagfors for kindly offering useful comments and suggestions. The National Astronomy and Ionosphere Center (Arecibo Observatory) is operated by Cornell University under a cooperative agreement with the National Science Foundation (NSF) and with support from the National Aeronautics and Space Administration (NASA). One of us (I. I. S.) was supported in part by both NASA and NSF.

APPENDIX

EVALUATION OF GRAIN-CLOUD PARAMETERS

By making some assumptions, it is possible to relate the measured total radar cross section of a cloud of particles in the vicinity of a cometary nucleus to the total mass of particles, the rate of mass loss from the nucleus due to these particles, and the observed continuum thermal emission from the particles at radio wavelengths. The need for these assumptions arises from our lack of knowledge of the physical nature and scattering properties of the particles ejected from cometary nuclei, their size and velocity distribution at ejection, and the history after ejection of each particle, which is undoubtedly size-dependent. In view of our lack of knowledge of all of these variables, we adopt a very crude model which assumes that (1) the particles are spherical and composed of a material with density ρ and dielectric constant ϵ; (2) the particles have a size distribution given by $n(a) \propto a^{-\alpha}$ ($\alpha > 0$), where n is the number of particles and a is their radius; (3) the rate, $\dot{n}(a)$, of particle ejection from the nucleus is time-independent; (4) the velocity of ejection is the so-called terminal velocity V_t (see Harmon *et al.* 1989); (5) an ejected particle continues to move with velocity V_t relative to the nucleus; and (6) this particle contributes fully to the radar cross section at the epoch of the observations if it is then within a cylinder whose surface coincides with the outer boundary of the "main beam" of the Arecibo radar at the epoch of the radar observations; otherwise, the particle's contribution to the radar cross section is zero. For an isotropic distribution of velocities of ejected particles, each with speed V_t, it follows that in this steady state situation the effective number of particles of radius a that would contribute to the radar cross section would be $n(a)\tau(a)$, where $\tau(a)$ is the average time interval for a particle of radius a to travel from the nucleus to the surface of the hypothetical cylinder of radius b whose axis intersects the nucleus and lies in a direction parallel to the line of sight from the radar:

$$\tau(a) = \frac{\pi b}{2V_t(a)} . \tag{A1}$$

I. TOTAL MASS

The total mass and radar cross section of a population of spherical particles with size distribution $n(a)$ and mass density ρ are given by

$$M = \tfrac{4}{3}\pi\rho \int_{a_0}^{a_m} n(a)a^3\, da , \tag{A2}$$

$$\sigma = \pi \int_{a_0}^{a_m} n(a)Q_b(a)a^2\, da , \tag{A3}$$

if multiple scattering is negligible. Q_b is the backscatter efficiency, and a_0 and a_m are the minimum and maximum particle radii in the distribution. In the Rayleigh approximation ($a \ll \lambda$) the backscatter efficiency for a spherical particle of dielectric constant ϵ is given by

$$Q_b(a) = C_Q a^4 , \tag{A4}$$

where

$$C_Q = 4\left(\frac{2\pi}{\lambda}\right)^4 \left|\frac{\epsilon - 1}{\epsilon + 2}\right|^2 .$$

Given our assumption of a power-law number distribution, we obtain

$$\begin{aligned} M &= \frac{4}{3}\sigma\rho C_Q^{-1}\left(\frac{7-\alpha}{4-\alpha}\right)\left(\frac{a_m^{4-\alpha} - a_0^{4-\alpha}}{a_m^{7-\alpha} - a_0^{7-\alpha}}\right) \\ &\cong \frac{1}{3}\sigma\rho\left(\frac{\lambda}{2\pi}\right)^4 \left|\frac{\epsilon+2}{\epsilon-1}\right|^2 \left(\frac{7-\alpha}{4-\alpha}\right)\left[1 - \left(\frac{a_0}{a_m}\right)^{4-\alpha}\right] a_m^{-3} , \end{aligned} \tag{A5}$$

provided that $a_0 \ll a_m$. If $\alpha = 4$ or 7, the integrations take a different form.

II. MASS-LOSS RATE

The mass-loss rate $\dot{M}$ for our model of time-independent particle ejection is given by

$$\dot{M} = \tfrac{4}{3}\pi\rho \int_{a_0}^{a_m} \dot{n}(a)a^3 da , \tag{A6}$$

$$\sigma = \pi \int_{a_0}^{a_m} \dot{n}(a)\tau(a)Q_b(a)a^2 da , \tag{A7}$$

where

$$V_t = C_v a^{-1/2}(1 - a/a_m)^{1/2} , \tag{A8}$$

with

$$C_v = [(3/2)V_g \dot{\mu} R \rho^{-1}]^{1/2}$$
$$= [(8/3)\pi \rho_n G]^{1/2} R a_m^{1/2} .$$

Here V_g is the gas thermal velocity, $\dot{\mu}$ is the mass flux of gas at the surface, ρ_n is the nucleus mass density, G is the gravitational constant, and R is the nucleus radius. With $\dot{n}(a) \propto a^{-\alpha}$, then from equations (A6)–(A8) for $\alpha \neq 4$ we have

$$\dot{M} = \frac{8}{3}\sigma\rho R\left[\left(\frac{8\pi}{3}\right)\rho_n G\right]^{1/2} a_m^{9/2-\alpha}\left[1-\left(\frac{a_0}{a_m}\right)^{4-\alpha}\right]\left[\pi b(4-\alpha)\int_{a_0}^{a_m}\frac{a^{5/2-\alpha}Q_b(a)}{(1-a/a_m)^{1/2}}\,da\right]^{-1} . \quad \text{(A9)}$$

For the general case we must evaluate the integral in equation (A9) numerically. For the Rayleigh regime ($a < \lambda/2\pi$) we have $Q_b = C_Q a^4$, in which case the integral equals $B(1/2, 15/2-\alpha)C_Q a_m^{15/2-\alpha}$, where B is the beta function.

III. RADIO CONTINUUM FLUX

With multiple scattering neglected, the continuum flux density S from a particle population with size distribution $n(a)$ is given by the following modified version of the Rayleigh-Jeans law (see, e.g., Walmsley 1985):

$$S = \frac{2\pi kT}{\lambda_c^2 d^2}\int_0^{a_m} n(a)Q_a(a;\lambda_c)a^2\,da , \quad \text{(A10)}$$

where T is the assumed particle temperature, d is the geocentric distance of the particle population, and $Q_a(a;\lambda_c)$ is the absorption efficiency at the observing wavelength λ_c of a particle of radius a. Using equation (A3) for the radar cross section, letting $n(a) \propto a^{-\alpha}$, and assuming that the radio continuum and radar observations both encompass the same number of particles, we have

$$S = \frac{2kT\sigma}{\lambda_c^2 d^2}\frac{\int_0^{a_m} a^{2-\alpha}Q_a(a;\lambda_c)da}{\int_0^{a_m} a^{2-\alpha}Q_b(a;\lambda)da} , \quad \text{(A11)}$$

where λ is the radar wavelength (as distinct from the wavelength λ_c of the radio continuum observations).

REFERENCES

Altenhoff, W. J., Huchtmeier, W. K., Schmidt, J., Schraml, J. B., Stumpff, P., and Thum, C. 1986, *Astr. Ap.*, **164**, 227.
Campbell, D. B., Harmon, J. K., Hine, A. A., Shapiro, I. I., Marsden, B. G., and Pettengill, G. H. 1983, *Bull. AAS*, **15**, 800.
Divine, N., *et al.* 1986, *Space Sci. Rev.*, **43**, 1.
Feldman, P. D. 1986, *Eos, Trans. AGU*, **67**, 300.
Feldman, P. D., A'Hearn, M. F., and Millis, R. L. 1984, *Ap. J.*, **282**, 799.
Feldman, P. D., and Festou, M. C. 1985, *IAU Circ.*, No. 4115, ed. B. G. Marsden.
Festou, M. C., *et al.* 1986, *Nature*, **321**, 361.
Goldstein, R. M., Jurgens, R. F., and Sekanina, Z. 1984, *A.J.*, **89**, 1745.
Hanner, M. S. 1986, *Eos, Trans. AGU*, **67**, 300.
Hanner, M. S., Aitken, D. K., Knacke, R., McCorkle, S., Roche, P. F., and Tokunaga, A. T. 1985, *Icarus*, **62**, 97.
Harmon, J. K., Campbell, D. B., Hine, A. A., Shapiro, I. I., and Marsden, B. G. 1989, *Ap. J.*, **338**, 1071.
Hirao, K., and Itoh, T. 1986, *Nature*, **321**, 294.
Kamoun, P. G., 1983, Ph.D. thesis, Massachusetts Institute of Technology.
Kamoun, P. G., Campbell, D. B., Ostro, S. J., Pettengill, G. H., and Shapiro, I. I. 1982, *Science*, **216**, 293.
Kaneda, E., Hirao, K., Takagi, M., Ashihara, O., Itoh, T., and Shimizu, M. 1986*a*, *Nature*, **320**, 140.
Kaneda, E., Ashihara, O., Shimizu, M., Takagi, M., and Hirao, K. 1986*b*, *Nature*, **321**, 297.
Keller, H. U., *et al.* 1986, *Nature*, **321**, 320.
Mazets, E. P., *et al.* 1986, *Nature*, **321**, 276.
McDonnell, J. A. M., *et al.* 1986, *Nature*, **321**, 338.
Meier, R. R., and Keller, H. U. 1985, *Icarus*, **62**, 521.
Ostro, S. J. 1985, *Pub. A.S.P.*, **97**, 877.
Reinhard, R. 1986, *Nature*, **321**, 313.
Sagdeev, R. Z., *et al.* 1986, *Nature*, **321**, 262.
Sekanina, Z. 1987, *Nature*, **325**, 326.
Sekanina, Z., and Larson, S. M. 1984, *A.J.*, **89**, 1408.
Shapiro, I. I., Marsden, B. G., Whipple, F. L., Campbell, D. B., Harmon, J. K., and Hine, A. A. 1983, *Bull. AAS*, **15**,, 800.
Smith, B. A., Larson, S. M., Szego, K., and Sagdeev, R. Z. 1987, *Nature*, **326**, 573.
Tokunaga, A. T., Golisch, W. F., Griep, D. M., Kaminski, C. D., and Hanner, M. S. 1986, *A.J.*, **92**, 1183.
Vaisberg, O. L., *et al.* 1986, *Nature*, **321**, 274.
Walmsley, C. M. 1985, *Astr. Ap.*, **142**, 437.
Weissman, P. R., and Kieffer, H. H. 1981, *Icarus*, **47**, 302.
Wilhelm, K. 1987, *Nature*, **327**, 27.
Wycoff, S. 1986, *Eos, Trans. AGU*, **67**, 300.

D. B. CAMPBELL: Department of Astronomy, Cornell University, Ithaca, NY 14853

J. K. HARMON: Arecibo Observatory, P.O. Box 995, Arecibo, PR 00613

I. I. SHAPIRO: Harvard-Smithsonian Center for Astrophysics, 60 Garden Street, Cambridge, MA 02138